aurum

AURUM MÜHENDİSLİK SİSTEMLERİ VE MİMARLIK DERGİSİ
AURUM JOURNAL OF ENGINEERING SYSTEMS AND ARCHITECTURE

Cilt 10, Sayı 1 | Yaz 2026
Volume 10, No 1 | Summer 2026

ANALYSIS OF ERBIUM-DOPED FIBER AMPLIFIERS USED IN RING BACKBONE OPTICAL NETWORKS USING MACHINE LEARNING

Neda NADERİ[1], N. Özlem ÜNVERDİ[2]*

[1]Department of Electronics and Communication Engineering, Yildiz Technical University, Istanbul, Türkiye, neda.naderi@std.yildiz.edu.tr
(https://orcid.org/0009-0002-6922-8057)

[2]Department of Electronics and Communication Engineering, Yildiz Technical University, Istanbul, Türkiye, unverdi@yildiz.edu.tr
(https://orcid.org/0000-0002-3995-3410)

Received: 02.06.2026
Accepted: 04.06.2026
Published: 30.06.2026
*Corresponding author

Research Article
pp.89-103

DOI: 10.53600/ajesa.1957573

Abstract

This study investigates erbium-doped fiber amplifier placement in wavelength-division multiplexing ring backbone optical networks and evaluates whether machine-learning-guided screened search can improve feasibility-aware planning. Ring-8 to Ring-16 topologies were simulated under standard and heterogeneous scenarios using a physical layer model that includes received power, amplified spontaneous emission (ASE), nonlinear interference, and an enhanced Gaussian noise (EGN) inspired correction. Candidate amplifier masks were ranked with a no-leak screening model and refined through bounded local search. Random Forest delivered the best screening performance, reaching receiver operating characteristic area under the curve (ROC-AUC) values of 0.9971 in the standard dataset and 0.9379 in the harder dataset, while leave-one-topology-out validation showed robust generalization across unseen ring sizes. In scaling experiments, the improved screened strategy matched the exhaustive optimum feasible ratio through Ring-16 and became 7.44 times faster than exhaustive search at Ring-16. These findings show that machine learning can serve as an efficient and interpretable decision support layer for impairment-aware EDFA placement without replacing full physical layer simulation.

Keywords: Communication technologies, ring backbone optical network, erbium-doped fiber amplifier, wavelength-division multiplexing, machine-learning-assisted screened search

HALKA OMURGALI OPTIK AĞLARDA KULLANILAN ERBIYUM KATKILI FIBER KUVVETLENDIRICILERIN MAKINE ÖĞRENMESI ILE ANALIZI

Özet

Bu çalışmada, dalga boyu bölmeli çoğullamanın (Wavelength-Division Multiplexing, WDM) kullanıldığı halka omurgalı optik ağlarda erbiyum katkılı fiber kuvvetlendiricilerin (Erbium-Doped Fiber Amplifier, EDFA) yerleşimi incelenmiş ve makine öğrenmesi destekli tarama yaklaşımının uygulanabilirlik odaklı ağ planlamasına katkısı değerlendirilmiştir. Ring-8 ile Ring-16 arasındaki topolojiler, alınan güç, kuvvetlendirilmiş kendiliğinden yayılım (Amplified Spontaneous Emission, ASE), doğrusal olmayan girişim ve geliştirilmiş Gaussian gürültü (Enhanced Gaussian Noise, EGN) yaklaşımından yararlanılan düzeltmeyi içeren fiziksel katman modeli kullanılarak standart ve heterojen senaryolar altında çalışılmıştır. Aday kuvvetlendirici yerleşimleri, bilgi sızıntısı içermeyen bir tarama modeliyle sıralanmış ve ardından sınırlandırılmış yerel arama ile iyileştirilmiştir. Analizde, Rastgele Orman (Random Forest), standart veri kümesinde 0,9971 ROC-AUC (Receiver Operating Characteristic Area under the Curve, Alıcı Çalışma Karakteristiği Eğrisi Altındaki Alan) ve zorlu veri kümesinde 0,9379 ROC-AUC değeriyle en başarılı tarama performansını göstermiştir. Ayrıca bir topolojiyi dışarıda bırakarak yapılan doğrulama (leave-one-topology-out), modelin görülmemiş halka boyutları için de anlamlı biçimde genelleştirilebileceğini göstermiştir. Ölçekleme deneylerinde iyileştirilmiş taramalı strateji, Ring-16'ya kadar tam arama ile aynı uygulanabilirlik oranını sağlamış ve Ring-16'da tam aramadan 7,44 kat daha hızlı çalışmıştır. Elde edilen bulgular ile makine öğrenmesinin tam fiziksel katman benzetiminin yerini almadan, EDFA yerleşimi için verimli ve yorumlanabilir bir karar destek katmanı sunabileceği belirlenmiştir.

Anahtar Kelimeler: İletişim teknolojileri, halka omurgalı optik ağ, dalga boyu bölmeli çoğullama, erbiyum katkılı fiber kuvvetlendirici, makine öğrenmesi destekli tarama

1. Introduction

Optical backbone networks must be planned with physical impairments in mind because routing and wavelength decisions that appear acceptable at topology-level may still fail once loss, noise, and nonlinear penalties are accumulated along the path (Azodolmolky et al., 2009; Ramaswami, Sivarajan, & Sasaki, 2009). This need has become more pressing as wavelengthdivision multiplexing (WDM) transport has expanded toward open, disaggregated, and programmable optical systems in which credible quality-of-transmission estimation supports both offline planning and operational decision support (Ferrari et al., 2020; Curri, 2022). Within that broader setting, erbium-doped fiber amplifier (EDFA) placement remains a distinct optimization problem. Amplifiers restore signal power after span loss but also introduce amplified spontaneous emission, so gain planning and noise planning cannot be separated in multi-span optical transmission (Agrawal, 2010). Earlier studies showed that amplifier location affects both cost and quality of transmission (QoT) and that optimal placement depends on route structure, span heterogeneity, and network-wide interactions rather than on isolated link budgets alone (Ramamurthy, Iness, & Mukherjee, 1998; Ibrahimi et al., 2020; Pedro & Costa, 2018).

A second literature stream concerns machine learning (ML) for quality of transmission (QoT) estimation. Supervised models have been used to predict whether a candidate lightpath will satisfy service requirements before deployment, thereby reducing conservative prechecks and improving planning speed (Rottondi, Barletta, Giusti, & Tornatore, 2018; Pointurier, 2021). Surveys now treat QoT prediction as one of the most mature ML applications in optical networks, while emphasizing uncertainty, dataset construction, and generalization to unseen states (Musumeci et al., 2019; Ayassi et al., 2022; Maryam et al., 2022). As summarized in Table 1, the literature supports impairment-aware planning, EDFA placement optimization, and machine learning assisted QoT screening, while also showing that these strands are usually studied separately.

This study brings these strands together by treating ring-based EDFA placement as a feasibility screened search problem. Machine learning is not presented as a substitute for physical layer planning; rather, it is used as a decision support layer that ranks candidate amplifier masks before exact QoT evaluation. The study strengthens the analysis in four ways: (i) topology scaling is extended from Ring-8 and Ring-10 to Ring-8 through Ring-16; (ii) the local refinement stage is explicitly bounded by a fixed candidate budget; (iii) cross topology robustness is evaluated through leave-one-topology-out validation; and (iv) the GN based QoT layer now exposes an EGN-inspired correction factor to improve physical transparency.

Table 1. Selected literature and its relevance to the present study.

Study	Primary focus	Methodological contribution	Relevance here
Ramamurthy et al. (1998)	Amplifier placement	Formalizes amplifier placement as an optimization problem	Provides the historical basis for node-level EDFA siting
Azodolmolky et al. (2009)	Impairment aware planning	Shows why physical impairments must be included in design	Supports feasibilityaware planning rather than topology only design
Rottondi et al. (2018)	QoT prediction	Applies supervised learning to unestablished lightpaths	Offers the closest precedent for predeployment feasibility screening
Ibrahimi et al. (2020)	Network-wide EDFA cost/QoT trade-off	Optimizes amplifier placement under QoT constraints	Motivates network level rather than purely local placement decisions
Pointurier (2021)	ML for QoT estimation	Organizes ML-QoT tasks, errors, and uncertainty sources	Frames the present screening approach within the QoT-ML literature

2. Materials and Methods

This section outlines the network architecture, physical layer assumptions, EDFA placement strategies, screening dataset design, and evaluation protocol used to assess feasibility-aware planning across the tested ring topologies.

2.1. Network Architecture and Scenario Design

The studied architecture is a WDM ring backbone in which each node has two physical neighbors and each source destination pair can be served through clockwise or counterclockwise routing. EDFA placement is encoded as a binary node vector; therefore, an N-node ring yields 2^N candidate placement masks before any cardinality restriction is applied. The experiments cover Ring-8, Ring-10, Ring-12, Ring-14, and Ring-16. Two experimental regimes are used. The standard regime evaluates progressively longer spans and heavier channel loading under regular conditions. The harder regime adds heterogeneous stress through stricter optical signal-to-noise ratio (OSNR) margins, wider EDFA gain and noise-figure variation, span heterogeneity, and mixed-service settings.

2.2. GN-İnspired Qot Model and Feasibility Criteria

The physical layer uses a lightweight Gaussian noise (GN) inspired approximation that jointly evaluates attenuation, EDFA gain, amplified spontaneous emission (ASE) accumulation, and nonlinear interference (NLI). A route is considered feasible only when both received power and OSNR satisfy service-dependent thresholds.

To address the known NLI overestimation tendency of standard GN formulations, the model introduces an explicit enhanced Gaussian noise (EGN)-inspired correction factor in the NLI term. This addition should be interpreted as a tunable correction that improves physical transparency rather than as a substitute for a full EGN or split-step Fourier model.

2.3. EDFA placement strategies and bounded local refinement

Five strategies are evaluated: baseline, greedy, ML-screened, improved ML-screened, and optimum strategies. The baseline is a simple reference mask; greedy adds amplifiers sequentially at the node that gives the largest immediate feasible ratio improvement; optimum enumerates all admissible configurations within the tested search space; screened search ranks candidate masks by learned probability before exact QoT evaluation; and the improved screened strategy combines ranking with local refinement.

To remove ambiguity from the refinement procedure, the local search stage is explicitly parameterized. Starting from the seed mask, the algorithm evaluates bounded 1 bit flips and localized EDFA shift operations within a radius of two nodes. The refinement candidate budget is capped at 50 neighbors, making the behavior of the refinement stage reproducible and computationally transparent.

2.4. Screening Dataset Construction and Model Selection

Simulation outputs are converted into a no-leak screening dataset rather than a direct feasible/non feasible admission dataset. For each scenario topology group, admissible EDFA masks are exactly evaluated and labeled as screening_label when their feasible ratio lies within the near optimal region of that group. Features are limited to planning-time quantities such as topology size, span conditions, service descriptors, and mask structure descriptors. Post evaluation quality targets are excluded from training to prevent leakage.

Logistic regression, random forest, support vector machine, and gradient boosting were benchmarked. Although more than one family performed well, Random Forest provided the strongest overall combination of F1, ROC-AUC, PR-AUC, and cross topology robustness, and was therefore adopted as the primary screening model in the final pipeline.

2.5. Leave-One-Topology-Out Validation And Evaluation Metrics

In addition to conventional train test evaluation, leave-one-topology-out validation is used to assess cross topology generalization. In this protocol, the model is trained on all but one topology size and is then evaluated on the held out ring. This is stricter than an in family random split because the model must operate on an unseen network geometry. Table 2 summarizes the main parameter groups used in the simulation and screening pipeline and shows that the experimental design jointly captures topology size, physical layer conditions, service descriptors, and heterogeneous stress factors.

The reported metrics include feasible ratio, runtime, gap to optimum, accuracy, precision, recall, F1-score, receiver operating characteristic area under the curve (ROC-AUC), precision recall area under the curve (PR-AUC), and balanced accuracy for the leave-one-topology-out evaluation. Single class safeguards were included in the implementation so that undefined AUC values are handled explicitly when necessary.

Table 2. Main parameter groups used in the simulation and screening pipeline.

Parameter group	Representative variables	Purpose
Topology and budget	Ring-8 to Ring-16, max EDFA	Defines the current experimental search space and amplifier budget
Physical span conditions	Span length (km), channel count, channel penalty (dB)	Controls loss growth and loadingdependent impairment pressure
Amplifier and mask structure	EDFA gain (dB), EDFA noise figure (dB), EDFA count, density, spacing and cluster penalties, gap statistics, nearestEDFA coverage	Captures amplifier quality together with spatial placement geometry
Service descriptors	Traffic, modulation, required OSNR (dB), QoT model	Represents service-dependent QoT requirements and simulation context
Heterogeneous stress descriptors	OSNR margin (dB), gain spread (dB), noise-figure spread (dB), span spread (km), hot-link and hotspot parameters	Models more challenging scenario variation beyond the standard family
Learning target	Screening label	Supports candidate ranking rather than direct post-deployment admission
Evaluation metrics	Feasible ratio, runtime (s), PR-AUC, ROC-AUC, precision, recall, F1, balanced accuracy, gap to optimum	Supports joint assessment of planning quality and screening value

3. Results

This section presents the main empirical findings of the study, including screening model validation, leave-one-topology-out generalization, and topology scaling results under both standard and more challenging heterogeneous scenarios.

3.1. Screening Model Validation

The primary validation question is whether the screening model can identify promising amplifier masks for ranking inside the search loop. On the standard screening dataset, all four candidate families performed strongly, but Random Forest was the strongest overall model with an accuracy of 0.9741, an F1-score of 0.9680, a ROC-AUC of 0.9971, and a PR-AUC of 0.9959. Gradient Boosting was close, while Logistic Regression lagged behind the nonlinear models. As reported in Table 3, Random Forest achieved the strongest overall screening performance, especially in ROC-AUC and PR-AUC, which supports its use as the main ranking model in the final search pipeline. On the harder screening dataset, discrimination decreased as expected because the heterogeneous scenarios create a narrower feasible region and more difficult decision boundary. Even so, Random Forest remained the most reliable model in overall ranking quality with a ROC-AUC of 0.9379 and a PR-AUC of 0.9137, while Gradient Boosting achieved the highest raw accuracy but a lower recall oriented balance.

Table 3. Validation performance of candidate screening models.

Dataset	Model	Accuracy	F1	ROC-AUC	PR-AUC
Standard	Random Forest	0.9741	0.9680	0.9971	0.9959
Standard	Gradient Boosting	0.9716	0.9650	0.9957	0.9934
Standard	Support Vector Machine	0.9547	0.9438	0.9920	0.9867
Standard	Logistic Regression	0.8796	0.8543	0.9607	0.9462
Harder	Random Forest	0.8622	0.7973	0.9379	0.9137
Harder	Gradient Boosting	0.8755	0.7844	0.9271	0.9052
Harder	Support Vector Machine	0.8622	0.7864	0.8896	0.8749
Harder	Logistic Regression	0.8530	0.7416	0.8936	0.8643

3.2. Leave-One-Topology-Out Validation

Cross topology robustness was evaluated through leave-one-topology-out validation using Random Forest. On the standard dataset, the held out topology ROC-AUC values ranged from 0.9112 to 0.9713. The strongest transfer appeared for Ring-10, Ring-12, and Ring-14, while the held out Ring-16 case was the most difficult because it represented the largest extrapolation in topology size. Table 4 shows that the Random Forest model preserved meaningful cross topology discrimination under leave-one-topology-out validation, although the held out Ring-16 case remained the most challenging.

On the harder dataset, ROC-AUC values ranged from 0.8570 to 0.8945. The corresponding PR-AUC values remained between 0.8278 and 0.8681, indicating that the screening model retained meaningful ranking ability even under more restrictive operating conditions. These results support stronger cross topology evidence than an in family random split, while still being presented as a practical generalization test rather than a universal proof of out-ofdistribution robustness.

Table 4. Leave-one-topology-out validation results for the Random Forest screening model.

Dataset	Left-out topology	Balanced accuracy	ROC-AUC	PR-AUC	F1
Standard	Ring-8	0.8798	0.9552	0.9053	0.8366
Standard	Ring-10	0.8720	0.9713	0.9450	0.8235
Standard	Ring-12	0.8825	0.9674	0.9548	0.8576
Standard	Ring-14	0.8053	0.9693	0.9715	0.7591
Standard	Ring-16	0.8270	0.9112	0.7996	0.7767
Harder	Ring-8	0.7617	0.8570	0.8278	0.6920
Harder	Ring-10	0.8326	0.8880	0.8628	0.7556
Harder	Ring-12	0.7890	0.8945	0.8681	0.7264
Harder	Ring-14	0.8141	0.8756	0.8609	0.7604
Harder	Ring-16	0.8080	0.8883	0.8661	0.7485

3.3. Standard Topology Scaling Results

The standard scaling experiments now cover Ring-8 through Ring-16. At Ring-8 and Ring-10, all methods reached the same feasible ratio outcome. From Ring-12 onward, the baseline strategy fell behind, whereas GREEDY, ML_SCREENED, and ML_SCREENED_IMPROVED continued to match the exhaustive OPTIMUM feasible ratio. At Ring-16, for example, the baseline feasible ratio was 0.1889, while the other search strategies and the optimum all reached 0.2194. These feasible ratio trends are illustrated in Figure 1 and show that GREEDY, ML_SCREENED, and ML_SCREENED_IMPROVED remained aligned with the exhaustive optimum throughout the standard scenario family, whereas the baseline strategy fell behind as topology size increased.

The main difference in this regime is computational cost. ML_SCREENED_IMPROVED was slower than exhaustive search at Ring-8, but the crossover occurred at Ring-10 and the advantage grew with topology size. Relative to OPTIMUM, ML_SCREENED_IMPROVED became 1.36 times faster at Ring-10, 2.82 times faster at Ring-12, 4.83 times faster at Ring-14, and 7.44 times faster at Ring-16. The plain ML_SCREENED strategy was even faster, but the improved version is retained because it behaves more robustly in the harder scenario family. The corresponding runtime comparison is shown in Figure 2, where the computational advantage of the screened strategies becomes more visible as the ring size increases.

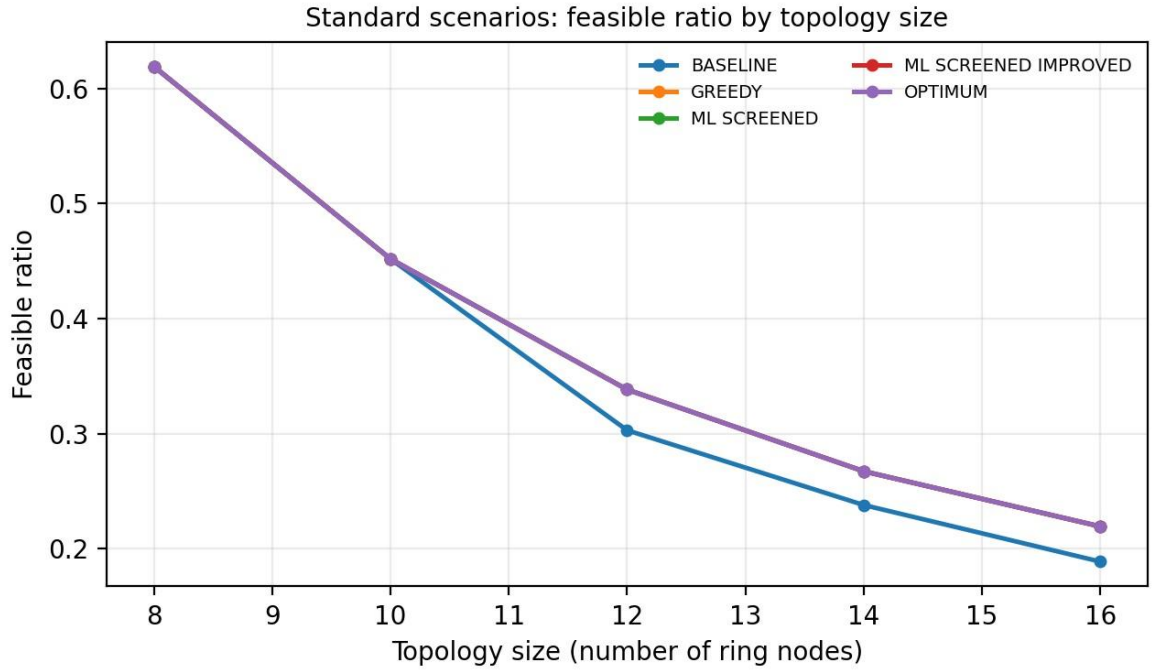

Figure 1. Feasible ratio curves across the standard scenario family.

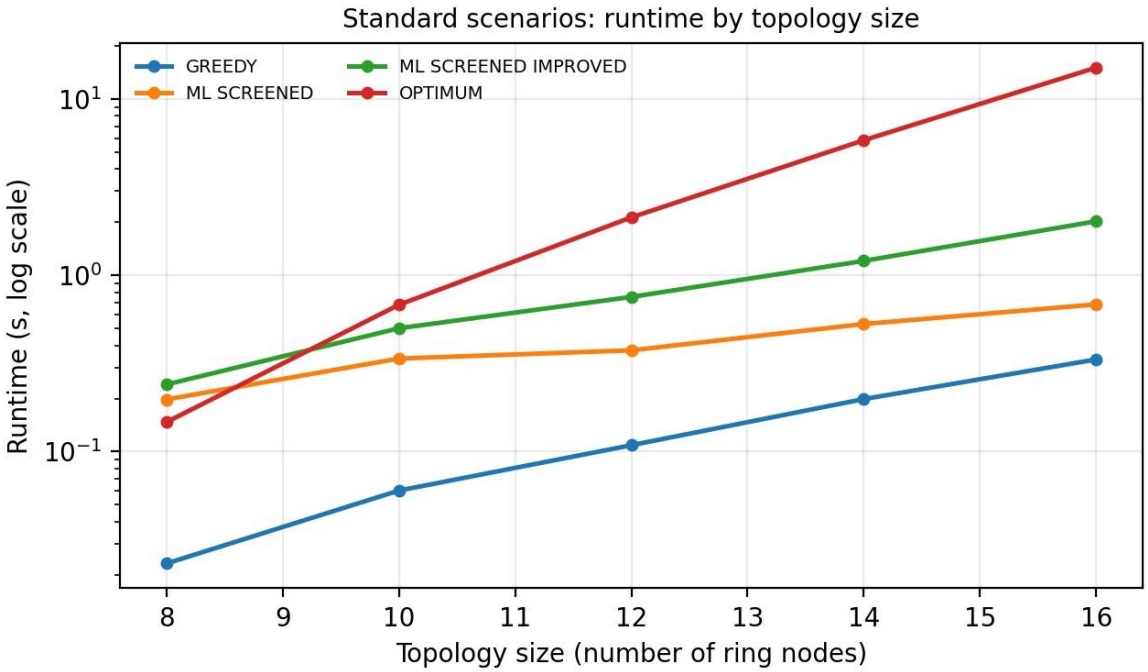

Figure 2. Runtime comparison across the standard scenario family.

3.4. More Challenging Heterogeneous Scenarios and Robustness

A second validation layer uses longer spans, higher channel loading, stricter OSNR thresholds, wider EDFA gain and noise-figure variation, and mixed service/modulation stress cases. Under this more challenging setting, feasible ratios drop sharply for all methods, confirming that the benchmark is materially more restrictive than the standard family. For instance, the optimum feasible ratio decreases from 0.1006 at Ring-8 to 0.0241 at Ring-16. As seen in Figure 3, the heterogeneous scenario family is considerably more restrictive, since feasible ratios decrease for all methods as operating conditions become harder.

The main result in this regime is the stability of the improved screened strategy. ML_SCREENED_IMPROVED matched the OPTIMUM feasible ratio at every tested topology size. GREEDY remained strong but showed small gaps at Ring-10 and Ring-12, while plain ML_SCREENED fell further behind at Ring-12. Runtime should be described cautiously: the improved screened method was not faster than exhaustive search on the smallest rings, but it reached runtime crossover by Ring-12 and became 1.56 times faster at Ring-14 and 2.13 times faster at Ring-16 while preserving optimum level feasible ratio performance. Figure 4 shows that ML_SCREENED_IMPROVED retains its practical value under harder conditions by reaching runtime crossover on larger rings while preserving optimum level feasible ratio performance.

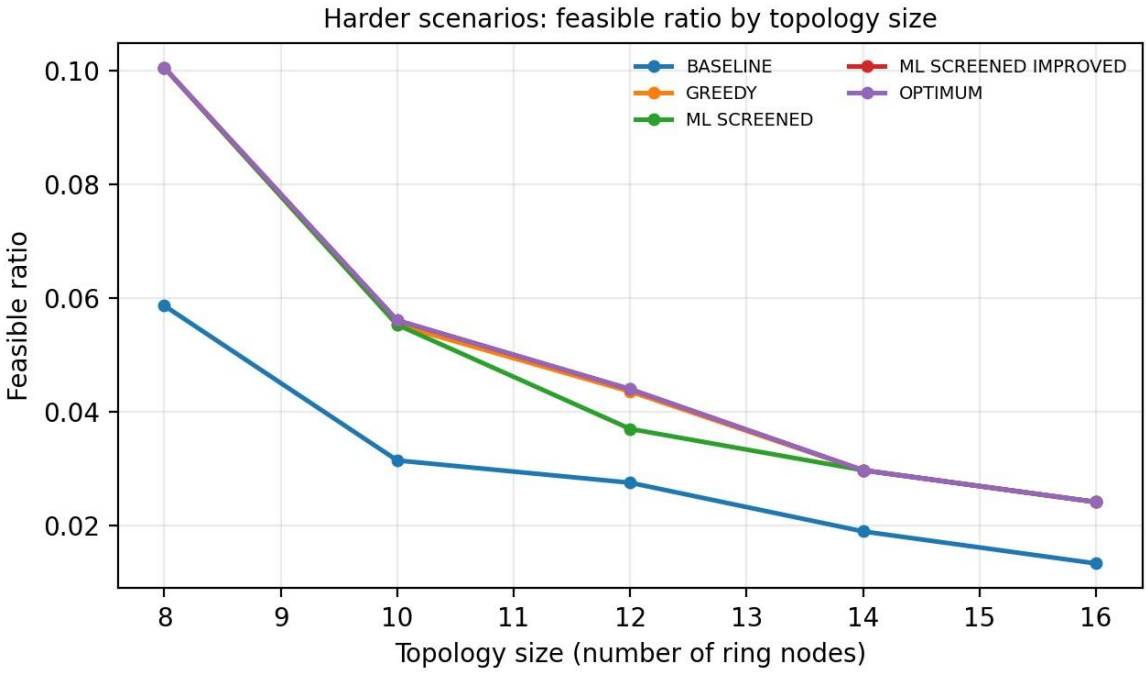

Figure 3. Feasible ratio curves for the harder heterogeneous scenario family.

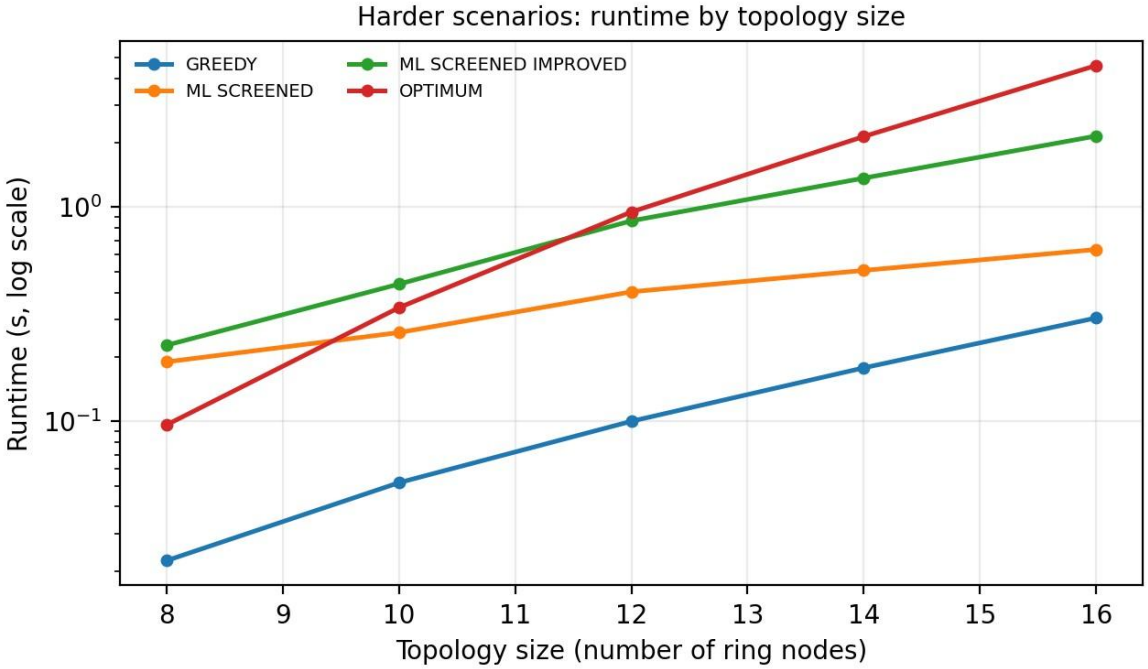

Figure 4. Runtime comparison for the harder heterogeneous scenario family.

3.5. Representative EDFA Placement Visualizations

To support visual interpretation of the EDFA placement decisions, Figures 5 through 8 present representative placement patterns for selected standard and heterogeneous scenarios. Figure 5 illustrates the standard Ring-8 case,

while Figure 6 shows how the placement pattern changes when the standard scenario is scaled to Ring-16. In the heterogeneous scenario family, Figure 7 presents the Ring-12 placement pattern and Figure 8 presents the corresponding Ring-16 case. Across these visualizations, the highlighted nodes indicate the EDFA locations selected by the OPTIMUM, ML_SCREENED_IMPROVED, and GREEDY strategies. These examples show that the proposed screening-based approach can produce placement patterns comparable to the exhaustive optimum under both standard and more challenging heterogeneous operating conditions.

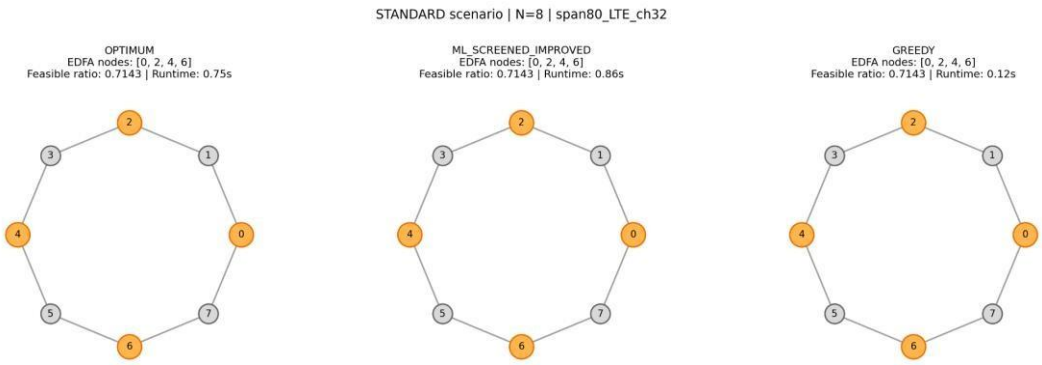

Figure 5. Representative EDFA placements for the standard scenario (Ring-8, span80_LTE_ch32).

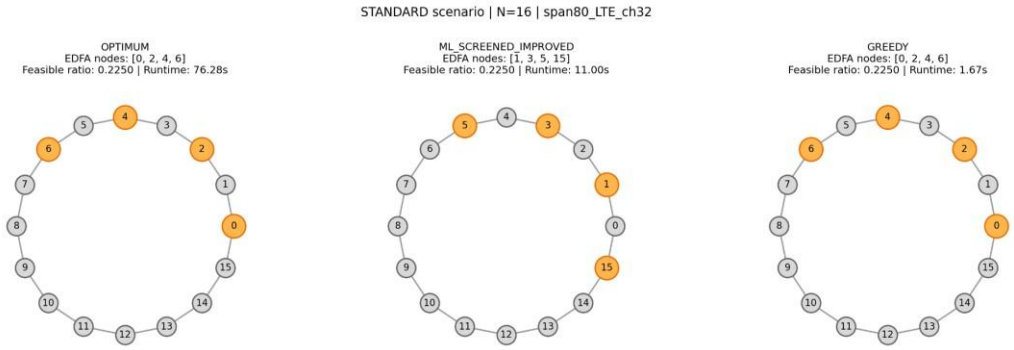

Figure 6. Representative EDFA placements for the standard scenario (Ring-16, span80_LTE_ch32).

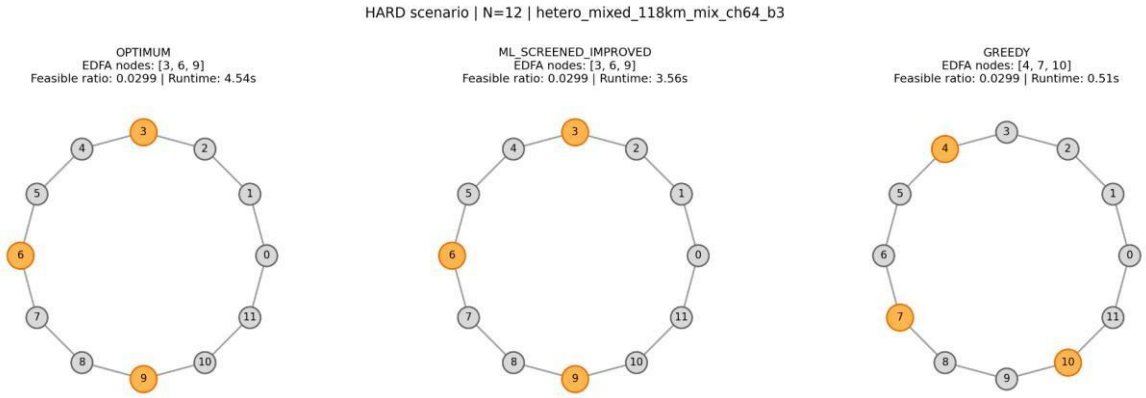

Figure 7. Representative EDFA placements for the heterogeneous scenario (Ring-12, hetero_mixed_118km_mix_ch64_b3).

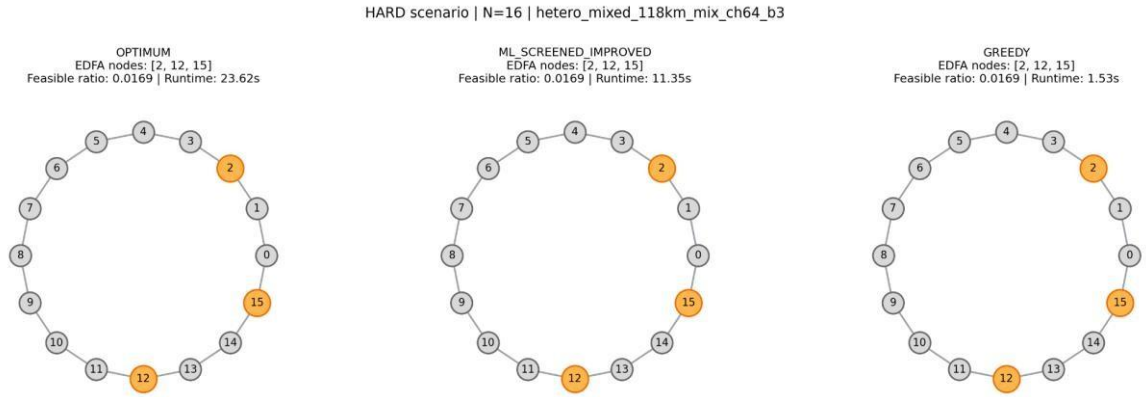

Figure 8. Representative EDFA placements for the heterogeneous scenario (Ring-16, hetero_mixed_118km_mix_ch64_b3).

4. Discussion

The findings position EDFA placement as more than a local link budget exercise. Once EDFA decisions are encoded at node-level and evaluated under received power and OSNR constraints, the planning space becomes both combinatorial and physically structured. That structure is precisely why a screening model can be useful: it removes clearly weak candidates before exact evaluation while preserving interpretability at the planning stage.

The results also clarify the role of machine learning in this paper. The primary contribution is not a standalone admission classifier; instead, it is an integrated planning framework in which a trained screening model assists search over amplifier placement masks. This places the work closer to decision support for impairment-aware optical planning than to generic computer science classification.

Several limitations still bound the scope of the study. The QoT layer is more realistic than a span-loss-only abstraction, but it remains lighter than full EGN, split-step Fourier, or fieldcalibrated models. The tested topologies are still ring structures whose symmetry may favor certain placement patterns. Leave-one-topology-out validation is substantially stricter than random splitting, yet it should still be interpreted as evidence of improved cross topology generalization rather than as a universal guarantee. Finally, the harder scenarios introduce useful heterogeneity, but they do not capture the full diversity of field traffic matrices, device aging, Raman effects, or measurement noise reported in uncertainty-oriented QoT work (Seve et al., 2018; Azzimonti et al., 2021; Maryam et al., 2022).

5. Conclusion

This study examined EDFA placement in wavelength-division multiplexing ring backbone optical networks under a Gaussian noise inspired QoT model and tested whether a trained screening layer can reduce the cost of feasibility-aware planning. The results show that EDFA placement becomes more consequential as span length, channel loading, service strictness, and heterogeneous stress increase. They also show that the planning problem can be reorganized as a screened search task without losing its physical interpretability, because all final feasibility decisions are still verified through the underlying physical layer model.

In the standard scenario family, GREEDY, ML_SCREENED, and ML_SCREENED_IMPROVED matched the exhaustive optimum feasible ratio across Ring-8 to Ring-16, while the baseline method fell behind on larger rings. In the more challenging heterogeneous scenarios, ML_SCREENED_IMPROVED matched the optimum feasible ratio at every tested topology size and became progressively more computationally attractive as the ring grew. The Random Forest screening model provided the most reliable overall validation and retained good leave-one topology-out performance on unseen ring sizes, which supports its use as the ranking layer in the final search pipeline.

Taken together, these findings highlight the practical importance of the study for impairmentaware optical network planning. Rather than replacing physics based analysis with a black box classifier, the proposed framework helps planners prioritize promising EDFA masks before exact evaluation, which becomes increasingly valuable as network size and scenario heterogeneity grow. In this sense, the study contributes a scalable and interpretable decision support approach for optical backbone design, especially in settings where many candidate configurations must be screened under realistic transmission constraints.

Future work should extend the framework toward non ring topologies, asymmetric traffic demands, richer physical layer models, and field-informed datasets while preserving the noleak screening design and the bounded refinement strategy. These extensions would help assess how well the same planning logic transfers to broader operational settings and would further strengthen the relevance of the approach for real network design workflows.

Acknowledgements

This project was supported by the Scientific Research Projects Coordination Unit (BAP) of Yildiz Technical University under project number FYL-2025-6850.

Conflict of Interest

The authors declare no conflict of interest related to this manuscript.

Author statement

This study is based on numerical simulation and machine-learning models derived from simulation outputs; therefore, ethical approval, consent to participate, and consent for publication are not applicable. No human participants, personal data, or animal experiments were involved. The simulation code, aggregated CSV tables, and generated figures are available from the authors upon reasonable academic request.

References

Agrawal, G. P. (2010). *Fiber-optic communication systems* (4th ed.). Hoboken, NJ: Wiley.

Ayassi, R., Triki, A., Crespi, N., Minerva, R., & Laye, M. (2022). Survey on the use of machine learning for quality of transmission estimation in optical transport networks. Journal of Lightwave Technology, 40(17), 5803-5815. https://doi.org/10.1109/JLT.2022.3184178

Azzimonti, D., Rottondi, C., Giusti, A., Tornatore, M., & Bianco, A. (2021). Comparison of domain adaptation and active learning techniques for quality of transmission estimation with small-sized training datasets. Journal of Optical Communications and Networking, 13(1), A56-A66. https://doi.org/10.1364/JOCN.401918

Azodolmolky, S., Klinkowski, M., Marin-Tordera, E., Careglio, D., Sole-Pareta, J., & Tomkos, I. (2009). A survey on physical layer impairments aware routing and wavelength assignment algorithms in optical networks. Computer Networks, 53(7), 926-944. https://doi.org/10.1016/j.comnet.2008.11.014

Curri, V. (2022). GNPy model of the physical layer for open and disaggregated optical networking [Invited]. Journal of Optical Communications and Networking, 14(6), C92-C104. https://doi.org/10.1364/JOCN.452868

Ferrari, A., Filer, M., Balasubramanian, K., Yin, Y., Le Rouzic, E., Kundrat, J., Grammel, G., Galimberti, G., & Curri, V. (2020). GNPy: An open source application for physical layer aware open optical networks. Journal of Optical Communications and Networking, 12(6), C31-C40. https://doi.org/10.1364/JOCN.382906

Ibrahimi, M., Ayoub, O., Musumeci, F., Karandin, O., Castoldi, A., Pastorelli, R., & Tornatore, M. (2020). Minimum-cost optical amplifier placement in metro networks. Journal of Lightwave Technology, 38(12), 3221-3228. https://doi.org/10.1109/JLT.2020.2991374

Maryam, H., Savva, G., Panayiotou, T., Tomkos, I., & Ellinas, G. (2022). Learning quantile QoT models to address uncertainty over unseen lightpaths. Computer Networks, 212, 108992. https://doi.org/10.1016/j.comnet.2022.108992

Musumeci, F., Rottondi, C., Nag, A., Macaluso, I., Zibar, D., Ruffini, M., & Tornatore, M. (2019). An overview on application of machine learning techniques in optical networks. IEEE Communications Surveys & Tutorials, 21(2), 1383-1408. https://doi.org/10.1109/COMST.2018.2880039

Pedro, J., & Costa, N. (2018). Optimized hybrid Raman/EDFA amplifier placement for DWDM mesh networks. Journal of Lightwave Technology, 36(9), 1552-1561. https://doi.org/10.1109/JLT.2017.2783678

Pointurier, Y. (2021). Machine learning techniques for quality of transmission estimation in optical networks. Journal of Optical Communications and Networking, 13(4), B60-B71. https://doi.org/10.1364/JOCN.417434

Ramamurthy, B., Iness, J., & Mukherjee, B. (1998). Optimizing amplifier placements in a multiwavelength optical LAN/MAN: The equally powered-wavelengths case. Journal of Lightwave Technology, 16(9), 1560-1569. https://doi.org/10.1109/50.712237

Ramaswami, R., Sivarajan, K. N., & Sasaki, G. H. (2009). Optical networks: A practical perspective (3rd ed.). Morgan Kaufmann.

Rottondi, C., Barletta, L., Giusti, A., & Tornatore, M. (2018). Machine-learning method for quality of transmission prediction of unestablished lightpaths. Journal of Optical Communications and Networking, 10(2), A286-A297. https://doi.org/10.1364/JOCN.10.00A286

Seve, E., Pesic, J., Delezoide, C., Bigo, S., & Pointurier, Y. (2018). Learning process for reducing uncertainties on network parameters and design margins. Journal of Optical Communications and Networking, 10(2), A298-A306. https://doi.org/10.1364/JOCN.10.00A298